The structure of the deposit produced by sedimentation of polydisperse suspensions

R. M. Dorrell,[1] A. J. Hogg,[1] E. J. Sumner,[2] and P. J. Talling[2]

Received 16 March 2010; revised 21 December 2010; accepted 28 December 2010; published 29 March 2011.

[1] To interpret the deposits from particle-laden flows it is necessary to understand particle settling at their base. In this paper a quantitative model is developed that not only captures how particles settle out of suspension but also the composition of the final deposit in terms of its vertical distribution of grain sizes. The theoretical model is validated by comparison to published experimental data that has been used to interpret the field deposits of submarine sediment-laden flows (Amy et al., 2006). The model explains two intriguing features of the experimental deposits that are also observed in natural deposits. First, deposits commonly have an ungraded, or poorly normally graded, region overlain by a strongly normally graded region. Second, the normalized thickness of the ungraded region increases as the initial concentration of the suspension is increased. In the theoretical model, the poorly normally graded region results from a constant mass flux into the bed that persists until the largest grain size present within the flow has been completely deposited. The effect of increasing the concentration of the initial suspension is to increase the thickness of the poorly graded part of the deposit and to decrease its average grain size. This work suggests that deposits with relatively thick, poorly graded bases can form from relatively high-concentration polydisperse suspensions, when the initial volume fraction of sediment is greater than approximately 20% and indicates that it is important to include these hindered settling effects in models of depositing flows.

Citation: Dorrell, R. M., A. J. Hogg, E. J. Sumner, and P. J. Talling (2011), The structure of the deposit produced by sedimentation of polydisperse suspensions, *J. Geophys. Res.*, *116*, F01024, doi:10.1029/2010JF001718.

1. Introduction

[2] Much of our understanding of geophysical flows that transport large volumes of sediment results from detailed analyses of their deposits. This is because many flows are hazardous and occur in inaccessible locations, making direct sampling of flows difficult or impossible. The deposits of flows, such as turbidity currents and pyroclastic surges, commonly contain distinctive vertical grading patterns; see, for example, *Gladstone and Sparks* [2002], *Sylvester and Lowe* [2004], and *Amy and Talling* [2006] and the discussion below (section 4.2). These flows include some of the most volumetrically important processes for moving sediment across the planet. Understanding the physical processes that generate these vertical grading patterns is fundamental to elucidating the dynamical behavior of flows from the deposits that they leave behind. It is therefore of practical use that models of the sedimentation process not only capture the settling behavior of the particles but also the structure of the resulting deposit, enabling comparison between modeling results and natural deposits.

[3] A first step in understanding the deposition from flows is to analyze the deposition from otherwise quiescent suspensions of particles. Previous work in this scenario has focused on sedimentation from suspensions of one or two particle sizes, rarely on truly polydisperse suspensions of particles and their deposits. Hindered settling laws for polydisperse suspensions [see, e.g., *Masliyah*, 1979; *Batchelor*, 1982; *Davis and Acrivos*, 1985] have been derived to take into account the effect of particle concentration on the effective fall velocity of a particle in a suspension. By limiting the physical complexity of the system to problems of particle sedimentation through an otherwise quiescent fluid, analytical solutions to an appropriate expression of mass conservation are obtainable for monodisperse suspensions, as first found by *Kynch* [1952] and more recently extended to bidisperse suspensions by *Dorrell and Hogg* [2010]. In these models, the quiescent fluid has no external mechanisms for maintaining particles in suspension. The only fluid motion is the upward flux of water generated by the downward settling particles. This upflux of water may have a resuspensive effect, noted in some experiments [*Amy et al.*, 2006], which decreases effective particle settling velocity, or for some slowly sedimenting particles, may carry these particles upward [*Dorrell and Hogg*, 2010].

[4] In this paper we present a model for the settling of polydisperse suspensions of noncohesive particles to calculate the sedimentation behavior and the structure of the

[1]Centre for Environmental and Geophysical Flows, School of Mathematics, University of Bristol, Bristol, UK.
[2]National Oceanography Centre, University of Southampton, Southampton, UK.

0148-0227/11/2010JF001718

resulting deposit. Theoretical results are compared to observations of the deposit structure of suspensions in the laboratory [*Amy et al.*, 2006]. This deposit structure is characterized by calculating the 10th, 50th and 90th percentiles of grain size of the deposit as a function of the normalized deposit height (which will henceforth be denoted by χ). These percentiles have been chosen to match field and experimental work on quiescent and turbulent settling problems [*Amy et al.*, 2006; *Talling et al.*, 2007]. *Amy et al.* [2006] suggested three different types of general deposit structure, which occur as the initial mass loading of particles in suspension, expressed as the initial depth-averaged volume fraction Θ, is varied. For low volume fractions ($0 < \Theta \leq 0.2$) strong segregation was observed, with the lowermost part of the deposit composed of a higher proportion of faster sedimenting particles than in the initial suspension. This lowermost part of the deposit was itself typically strongly graded up until $\Theta \approx 0.1$, at which point grading became less pronounced. Increasing the mass loading ($0.2 < \Theta \leq 0.5$) progressively decreased this segregation until the distribution of the deposit, throughout its entire height, was roughly equivalent to the distribution of the initial suspension. The latter was observed for $0.5 < \Theta \leq \phi_m$, where ϕ_m is the maximum packing concentration.

[5] While *Amy et al.* [2006] investigated suspensions with varying mixtures of kaolinite clay and silica sand, we focus on the results for suspensions of only sand with no clay content; thus, we assume that the suspensions have no cohesive forces. Further, from now on, we assume that particles are all of the same density and shape so that the settling velocities are solely a monotonic function of particle size. This assumption could be relaxed within the theoretical framework described below to include particles of varying density and size, but it is a useful simplification because it allows us to discuss sedimentation and segregation in terms of particle size alone. It should also be noted that in the experiments of *Amy et al.* [2006], and in the model described below, the suspensions are assumed to be initially well mixed vertically with no stratifications in concentration such as those that might occur in decelerating shear flows.

[6] The mathematical model presented in this study will be shown to reproduce the graded and ungraded regions observed in the experimental deposits of *Amy et al.* [2006]. Similar grading patterns are also commonly observed in the deposits of submarine flows (section 4.2). While the model presented here is for the simplified case of deposition in a quiescent fluid, thus preventing direct comparison with submarine flow deposits, some of the insights that it provides may explain features observed in natural deposits.

[7] The paper is structured as follows. First we derive the mathematical model for settling polydisperse suspensions and highlight some of its key features (section 2.1) and present the numerical method that will be employed for integrating the coupled system of governing equations (section 2.2). Results are given in section 3, first deriving general relationships between the composition of the deposit and the overlying suspensions (section 3.1) and then presenting results from numerical integration of the equations that are compared directly to previously reported experimental measurements [*Amy et al.*, 2006] (section 3.2). In section 3.3 we develop an approximate solution to the governing equations that captures accurately the composition and extent of the ungraded portion of the deposit. Our results are discussed in section 4, where we provide simple interpretations of the phenomena, analyze the performance of the model as the polydisperse suspension is represented through a varying number of discrete classes of particles (section 4.1) and suggest some implications for naturally occurring flows (section 4.2). Finally, we draw some brief conclusions (section 5).

2. Mathematical Models of Polydisperse Suspensions of Particles

2.1. Formulation

[8] The settling speed of a solitary spherical particle of sufficiently small diameter, d, in an unbounded and otherwise quiescent fluid domain is given by Stokes's settling law [see, e.g., *Batchelor*, 1967; *Soulsby*, 1997]

$$w(d) = \frac{g(\rho_s - \rho_f)d^2}{18\mu}, \tag{1}$$

where ρ_s and ρ_f are the solid and fluid densities, respectively; g denotes gravitational acceleration; μ is the dynamic viscosity of the fluid; and d is the particle diameter. However this expression is strongly modified by the nearby presence of suspended particles, which generate an upward "return" flow of interstitial fluid as they settle and which may enhance the effective viscosity of the interstitial fluid.

[9] In what follows it will be assumed that the concentration varies only along this vertical axis, measured upward, normal to the bed and denoted by z, with the suspension assumed to be homogenous in the plane tangential to the bed. The horizontal surface $z = 0$ corresponds to the impermeable surface that underlies the suspension, while $z = h$ corresponds to the initial upper interface between the top of the suspension and the surrounding fluid. The interface between the deposit and the overlying suspension occurs at $z = \eta(t)$. We define $\phi_i(z, t)$ to be the concentration of the ith particle class and $\Phi(z, t) = \sum_{i=1}^{N} \phi_i$ to be the sum of concentrations over all N particle classes. We thus find that the initial depth-averaged concentration of particulate matter in the sedimenting suspension is given by

$$\Theta = \frac{\int_0^h \Phi(z,0)\mathrm{d}z}{h}, \tag{2}$$

and mass conservation implies that Θ is temporally invariant. Mass conservation also implies that the net vertical flux of matter vanishes at each point and thus denoting the settling velocities of each class of particle species by W_i and of the fluid by w_f, we find that

$$(1 - \Phi)w_f + \sum_{i=1}^{N} \phi_i W_i = 0. \tag{3}$$

This may be rewritten in terms of the slip velocity of each class of particles ($w_{pi} = W_i - w_f$),

$$W_i = w_{pi} - \sum_{j=1}^{N} \phi_j w_{pj}. \tag{4}$$

Then following *Masliyah* [1979] and *Lockett and Bassoon* [1979] we enforce a local balance of forces on individual particles between the submerged weight ($\frac{\pi}{6}(\rho_{si} - \rho_f)gd_i^3$) and the viscous drag $3\pi\mu_e w_{pi} d_i$, where ρ_{si} and d_i denote the density and diameter of the particles in class i, respectively; μ_e denotes the effective viscosity; and in these expressions the particles have been assumed to be spherical. Thus we deduce $w_{pi} = w(d_i)\mu/\mu_e$. This balance of forces is applicable provided the concentration of particulate is less than the maximum for which a suspension can be attained, ϕ_m, and in which case the particles are not in contact. If the volume fraction were to exceed ϕ_m, then the submerged weight of the particles would be carried by normal reaction forces through the particle contacts and the particles would no longer sediment. The maximum packing concentration is assumed to be a constant, $\phi_m = 0.6$, chosen as the limit of particle sedimentation, observed by *Amy et al.* [2006]; this assumption significantly simplifies the analysis that follows. It is to be expected that the maximum packing fraction of polydisperse suspensions will vary with the distribution of particle sizes and relative volume fractions of each species of particles [*Kansal et al.*, 2002; *Shapiro and Probstein*, 1992]. However, we neglect this variation, anticipating that it will only have a relatively weak effect on the results [*Dorrell and Hogg*, 2010]. Finally to complete the model, we assume that the enhancement to the viscosity is given by $\mu_e = \mu(1 - \Phi)^{-n}$, with parameter $n = 5$ [see, e.g., *Davis and Gecol*, 1994]. Together this formulation yields expressions for the settling velocities of each class of particles, W_i, as first developed by *Masliyah* [1979] and *Lockett and Bassoon* [1979]; this description will be henceforth termed the MLB model of settling velocities and it is given by

$$W_i = \begin{cases} -(1-\Phi)^{n-1}\left(w(d_i) - \sum_{j=1}^{N} \phi_j w(d_j)\right) & \phi < \phi_m \\ 0 & \phi \geq \phi_m. \end{cases} \quad (5)$$

We note that it recovers the commonly used expression for the hindered settling velocity of monodisperse suspensions when $N = 1$, as developed by *Richardson and Zaki* [1954], but that it is now extended to polydisperse suspensions. As shown by *Dorrell and Hogg* [2010], it is important to use a discontinuous form of settling velocities if the focus of study is on the structure of the deposit; without it, the suspensions are not predicted to settle out completely within finite time. In (5) we use Stokes' settling velocity formula (1) to determine $w(d_i)$, an assumption that is reasonable provided the particles are sufficiently small. This formulation could be easily generalized by the inclusion of an empirical expression for settling velocities in unbounded domains, appropriate to larger particles or particles of different shapes [*Dietrich*, 1982; *Soulsby*, 1997].

[10] Mass conservation for the ith particle class is expressed by

$$\frac{\partial \phi_i}{\partial t} + \frac{\partial}{\partial z}(W_i \phi_i) = 0. \quad (6)$$

This equation is solved subject to an initial constant concentration profile, $\phi_i(z, 0) = c_i$, and a no flux condition at the impermeable boundary underlying the suspension $\phi_i(0, t)W(\phi_i(0, t)) = 0$. A consequence of this model for the evolution of the concentration fields, ϕ_i, is that there may exist discontinuous jumps (shocks) in particle concentration in the suspension. These shock speeds $\dot{S}$, are given by the Rankine-Hugoniot condition

$$\dot{S} = \frac{\phi_i^- W_i^- - \phi_i^+ W_i^+}{\phi_i^- - \phi_i^+} \quad (7)$$

in terms of the concentrations and settling velocities above, ϕ_i^+, W_i^+, and below, ϕ_i^-, W_i^-, the shock, respectively. Since the evolution equations are coupled, the presence of a shock implies simultaneous discontinuities in the volume fractions of all the species, or discontinuities in their gradients, and the expression for $\dot{S}$ may be formulated for each species. For bidisperse suspensions, sedimentation behavior can be classified in terms of the existence and the location of these shocks [*Dorrell and Hogg*, 2010]. Further the shock equation (7) models the bed growth rate, $\dot{\eta}$, where the total concentration beneath the shock Φ^- is equal to the maximum packing fraction, ϕ_m, and the associated sediment flux vanishes.

[11] Figure 1 gives a schematic of the sedimentation process and time evolution of a polydisperse suspension of particles of different sizes in a cell with impermeable solid vertical walls. As is shown, from an initially well mixed suspension at time t_0 the suspension begins to separate into $N + 2$ different regions (t_1), where N is the total number of particle classes. At the bottom of the cell there is a stationary deposit of height η, initially composed of a mix of particles of all sizes, at the top of the cell is a region of clear fluid with no particles present. Between these two are N other regions of sedimenting particles. An interface, γ_1, separates the clear fluid and the suspension. Then below γ_1 there are further interfaces, γ_i ($2 \leq i \leq N - 1$), such that particle classes from $1 \leq j \leq i$ are found between interfaces γ_i and γ_{i+1}. Finally at the base of the flow, but above the deposited material, there is a region in which all of the particle classes are present. In these internal regions of the suspension, the particle concentration may vary through concentration shocks and rarefaction fans (see *Dorrell and Hogg* [2010] for bidisperse suspensions), while the interfaces between them are given by discontinuous changes ("shocks") in the concentration fields. Indeed from (7), it can be seen that the velocity of γ_i is $W_i(\phi^-)$.

[12] By some later time t_2 the largest particle class, found only in the lowermost settling region will have been completely deposited (see Figure 1). Up until this point the flux in to the base has remained constant, set by the distribution of particles in the lowermost settling region. Afterward the flux of particles in to the base will change as different settling regions are deposited (see the Figure 1 at times t_3 and t_4). The deposit structure thus switches from ungraded to graded when the largest particle class has been completely deposited, as will be discussed later. Finally, at some time t_5, when the top interface meets the bottom interface, all particles have been deposited.

2.2. Numerical Computation

[13] The sedimentation of suspensions of a continuous distribution of particle sizes is approximated by discretizing the distribution into N separate classes and computing the evolution of each class of particles. This entails numerically integrating N coupled equations (equation (6)), each of

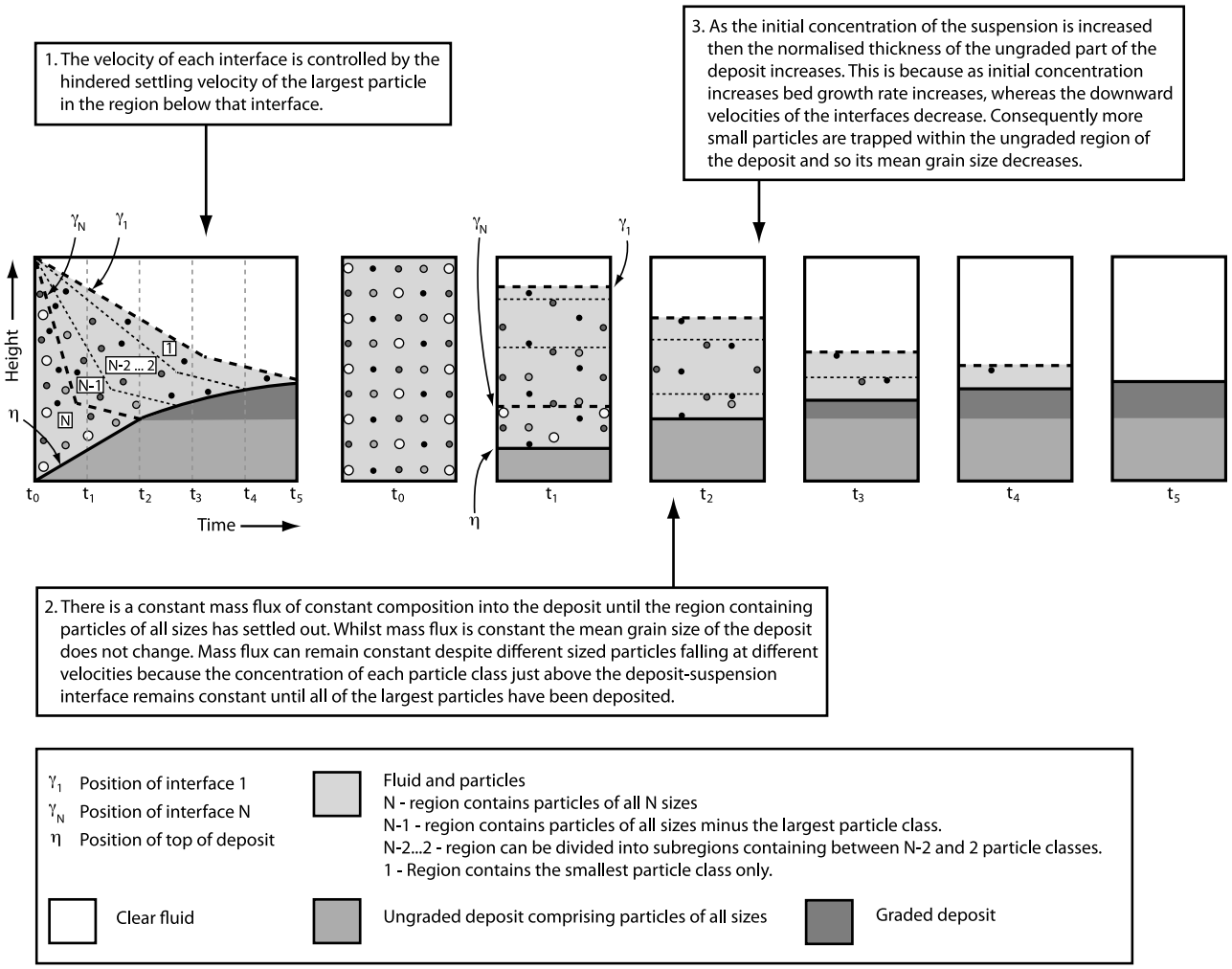

Figure 1. Sketch showing the sedimentation behavior of a polydisperse suspension of particles for varying times, T. The initial well-mixed suspension develops $N + 2$ distinct regions: the deposit at the bottom of the suspension, a region of clear fluid above the suspension, and N regions containing particles. The first region of particles contains only the smallest size and slowest settling class of particles; the second region contains the two smallest classes, etc.; and the Nth region contains particles of all sizes.

which expresses mass conservation of a particular species. Our numerical method employs the algorithm developed by *Bürger et al.* [2008, scheme 10] for discontinuous settling laws (equation (5)), which resolves shocks without the need for separate attention. This algorithm is formally accurate to second order away from shocks in particle concentration. In the numerical computation reported here, the number of classes was set at $N = 28$ with a spatial step size of $\Delta z = h/2000$ and a modified version of the Courant condition was used to give the time step, $\Delta t = \Delta z/[1.25 \max(|W_i|)]$ [*Bürger et al.*, 2008].

[14] In Figure 2 we present the numerical results for the evolution of the total concentration field, $\Phi(z, t)$, from an initial condition with $\Theta = 0.3$. For this computation the polydisperse suspension has been represented by $N = 28$ classes (see Figure 3a). This results in distinct steps in the particle concentrations field, $\Phi(z, t)$, which are visible in each of the profiles plotted in Figure 2. These steps correspond to the interfaces between regions of different particle distributions in the suspension.

[15] Polydisperse suspensions undergo similar settling behavior as monodisperse and bidisperse suspensions with the possibility of developing complex interior structures [*Dorrell*, 2010; *Dorrell and Hogg*, 2010]. The main focus of this paper is the resulting character of the final structure of the deposit and thus the numerical calculations were allowed to run until sedimentation was complete, after which time deposit structure was analyzed. The structure of the deposits that arises from the sedimentation of a bidisperse suspension, settling from an initially well-mixed suspension, was analyzed by *Dorrell and Hogg* [2010]. The deposits from polydisperse suspensions share some of these features: they comprise a basal layer of ungraded particles of both species, overlain by successive regions, each depleted of the successively largest particle and eventually overlain by a region containing only particles with the slowest settling velocity. As has been described above, this structure is formed because there is a constant flux of each class of particles through the shock (a discontinuous increase) in particle concentration to the bed, until all of the largest particles

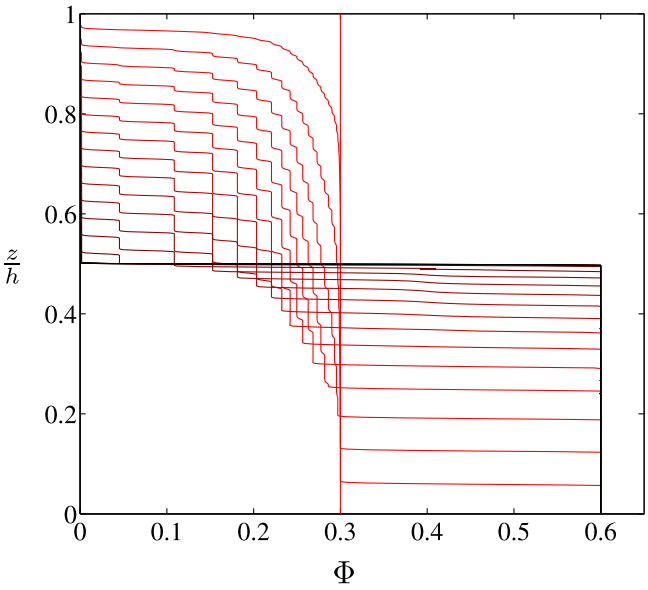

Figure 2. The total concentration of particles, Φ, as a function of the normalized depth, z/h, at various instants of time. The profiles are computed numerically from the initial distribution of particles sizes plotted in Figure 3a with an initial volume fraction of the suspension, $\Theta = 0.3$. Concentration profiles are shown at dimensionless time steps $\Delta T = 2$ from $T = 0$ to $T = 40$, where $T = ht/|w(d_N)|$.

have been deposited. This results in an ungraded deposit. Thereafter a change in deposition rate occurs because all of the largest particles have been deposited and the grain size decreases with height in the deposit.

[16] The structure of the deposit is strongly dependent on the total amount of sediment initially in suspension [cf. *Dorrell and Hogg*, 2010; *Amy et al.*, 2006]. Increasing the initial depth-averaged, total volume fraction of the suspension, Θ, increases the depth of the ungraded basal layer, when normalized with respect to the final deposit depth, χ. Increasing Θ also implies that the depth of the deposit increases. Furthermore, as the total volume fraction increases, the amount of particulate material in the largest class of particles increases. Above we showed that an ungraded deposit is formed until the largest class of particles is deposited and thus it is to be expected that the depth of the ungraded portion of the deposit also grows as the total concentration of particles is increased. However, this does not explain the growth of the depth of the ungraded basal layer when normalized with respect to final deposit depth. To explain the increase we observe that with increasing initial mass loading the proportion of smaller particles found in the ungraded, basal region of the deposit must also increase. A direct consequence of this is that the mean, concentration weighted, grain size of the ungraded basal part of the deposit must decrease.

3. Results

[17] Before presenting the results of numerical integrations of the governing equations that may be compared directly to experiments, we first deduce results about the composition of the ungraded portion of the deposit and its relationship to the overlying suspension.

3.1. Theoretical Analyses

[18] A major interest of this study is the determination of how the grain size distribution within the deposit is related to the initial grain size distribution of the suspension, and in this section we analyze what may be predicted from the theoretical model (section 2.1). In particular we analyze the instantaneous relationship between the composition of the suspension just above the deposit and the composition at the top of the deposit. To measure the state of the suspension and deposit, we define the following volume fraction weighted average of the unhindered settling velocity, $\overline{w}$, which is given by

$$\overline{w} = \frac{\sum_{i=1}^{N} \phi_i w(d_i)}{\sum_{i=1}^{N} \phi_i}, \tag{8}$$

and this overbar notation will be used elsewhere to denoted the volume fraction weighted average. We note that if the particles are of equal density and are sufficiently small so that their settling velocity is given by (1), then this quantity, $\overline{w}$ is proportional to the volume fraction weighted average of the square of their diameter $\overline{w} \propto \overline{d^2}$. As above, we focus the discussion on this scenario in which all of the particulate matter is of the same density and shape so that an increased average settling velocity is equivalent to an increased average grain size.

[19] First, we demonstrate that $\overline{w}$ is always increased across shocks to the maximum packing fraction, recalling the bed growth rate is given by the speed of this shock (equation (7)). This means that the average grain size in the deposit is always greater than or equal to the average grain size in suspension immediately above it. This result may be established by manipulating the shock conditions that express conservation of mass between states above and below the shock, denoted by the superscript plus and minus, respectively. Considering then expressions for the conservation of mass of a single species, (7), we may write the rate of growth of the bed, $\dot{\eta}$, as

$$\dot{\eta} = \frac{\phi_i^+ (1-\Phi^+)^{n-1} \left(w(d_i) - \sum_{j=1}^{N} \phi_j^+ w(d_j) \right)}{\phi_i^- - \phi_i^+}, \tag{9}$$

in terms of the ith particle species. As $\dot{\eta}$ is independent of the particle class used in (9), we also find

$$\dot{\eta} = \frac{\sum_{i=1}^{N} \phi_i^+ (1-\Phi^+)^{n-1} \left(w(d_i) - \sum_{j=1}^{N} \phi_j^+ w(d_j) \right)}{\phi_m - \Phi^+} = \frac{(1-\Phi^+)^n \sum_{i=1}^{N} \phi_i^+ w(d_i)}{\phi_m - \Phi^+}, \tag{10}$$

given that the sum of the individual particle concentrations within the deposit is equal the maximum packing concentration. In these expressions we have denoted the total volume fraction of particles above the shock by Φ^+ and have used the condition that there is vanishing mass flux within the deposit, because the particles are stationary. Eliminating

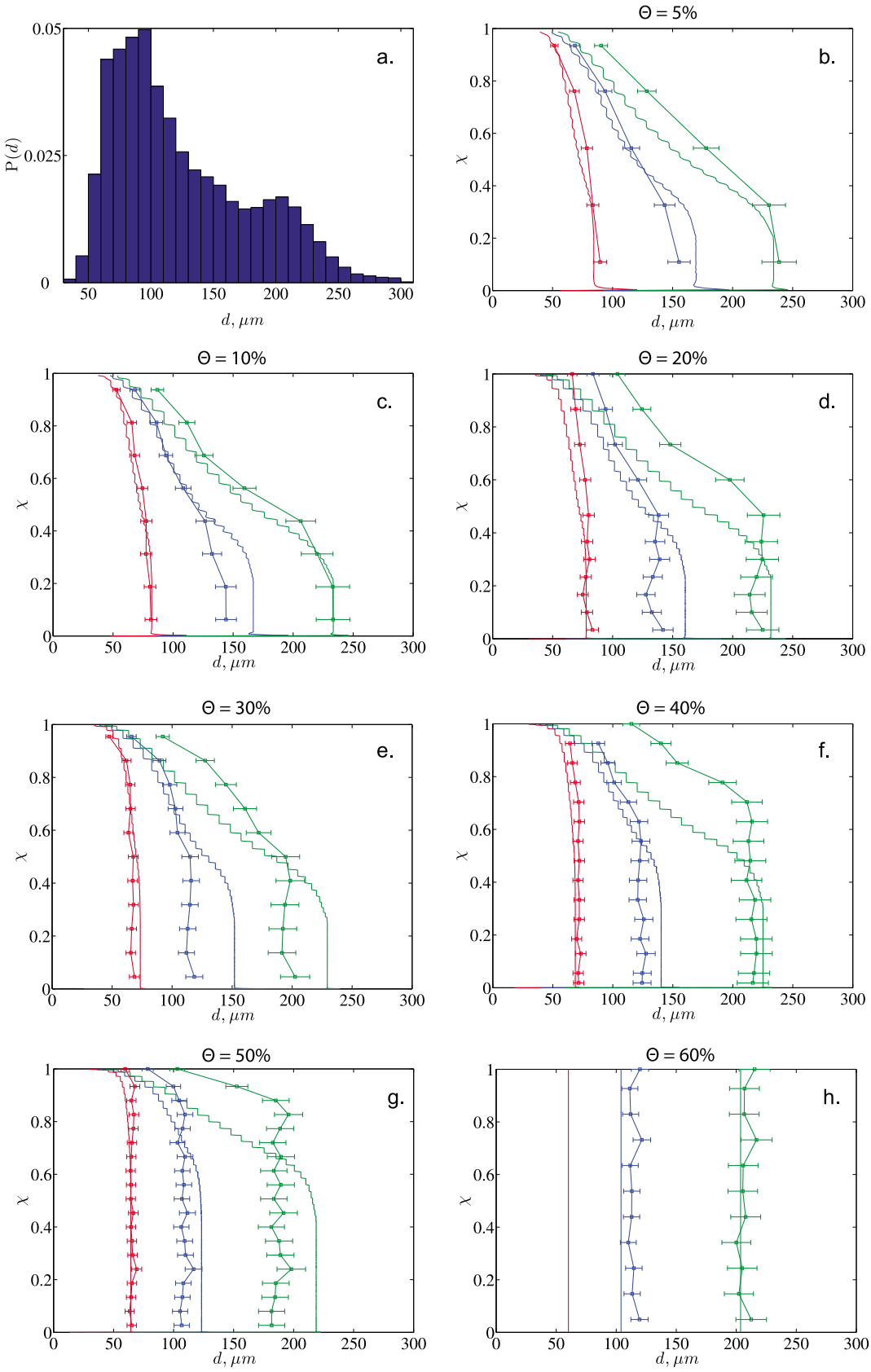

Figure 3

$\dot{\eta}$ from (9) and (10), we find that the volume fraction of an individual species within the deposit is given by

$$\phi_i^- = \phi_i^+ + \left(\frac{\phi_m - \Phi^+}{1-\Phi^+}\right)\frac{\phi_i^+\left(w(d_i) - \sum_{j=1}^N \phi_j^+ w(d_j)\right)}{\sum_{j=1}^N w(d_j)\phi_j^+}. \quad (11)$$

We may now calculate the composition of the deposit in terms of the overlying suspension. To this end, we calculate the average unhindered settling velocity of particles at the top of the deposit, $\overline{w^-}$, in terms of the unhindered settling velocity at the base of the suspension, just above the deposit, $\overline{w^+}$. We reiterate that if the particles are sufficiently small so that their unhindered settling velocities are given by Stokes's settling velocities, then this is equivalent to calculating the average of the diameter squared. Then calculating the average settling velocity, $\overline{w^-}$, we find that

$$\overline{w^-} = \frac{\Phi^+}{\phi_m}\frac{1-\phi_m}{1-\Phi^+}\overline{w^+} + \frac{1}{\phi_m}\frac{\phi_m - \Phi^+}{1-\Phi^+}\frac{\overline{w^{+2}}}{\overline{w^+}}. \quad (12)$$

Then we may deduce that

$$\overline{w^-} - \overline{w^+} = \frac{1}{\overline{w^+}}\frac{\phi_m - \Phi^+}{\phi_m(1-\Phi^+)}\left(\overline{w^{+2}} - \overline{w^+}^2\right) \quad (13)$$

$$= \frac{1}{\overline{w^+}}\frac{\phi_m - \Phi^+}{\phi_m(1-\Phi^+)}\overline{\left(w^+ - \overline{w^+}\right)^2} \geq 0. \quad (14)$$

Thus, the average grain size increases across shocks to the maximum packing fraction; in other words, the average grain size in the deposit must exceed the average grain size in the suspension immediately above it.

[20] Further we can show that the volume fraction of a particular class of particles relative to the total volume fraction, $(\phi_i/\sum_{j=1}^N \phi_j)$, is increased in the deposit over that in the suspension if the grain size of that particle class is greater than the average grain size ($w(d_i) > \overline{w^+}$) and vice versa. This is established using (11) from which we deduce

$$\frac{\phi_i^-}{\phi_m} - \frac{\phi_i^+}{\Phi^+} = \frac{\phi_i^+(\phi_m - \Phi^+)}{\phi_m\Phi^+(1-\Phi^+)\overline{w^+}}\left(w(d_i) - \overline{w^+}\right). \quad (15)$$

This relationship further implies that as the concentration within the suspension tends to the maximum packing ($\Phi^+ \rightarrow \phi_m$), then the volume fraction of each species within the deposit tends to its value in the suspension ($\phi_i^- \rightarrow \phi_i^+$) and consequently the average grain size within the deposit tends to the average grain size in the suspension ($\overline{w^-} \rightarrow \overline{w^+}$). The latter is established from (14), from which we deduce that $\overline{w^-} \rightarrow \overline{w^+}$ as $\Phi^+ \rightarrow \phi_m$, and since the average unhindered settling velocity is a proxy for the size of the particles, we deduce that the deposit and the suspension have an identical average particle size. Thus, in this limit of a highly concentrated suspension, the ungraded portion of the deposit includes an increased proportion of finer particles. A further consequence is that the depth of the ungraded region within the deposit must also increase as the volume fraction of the suspension increases. This is because the ungraded region persists until all of the largest particle class have settled out of suspension. Thus as the deposit at the maximum volume fraction, ϕ_m, contains a greater proportion of fine particles, the layer deposited must be of greater depth by the time all of the largest particles have settled out of suspension.

[21] These analyses show that the upper surface of the deposit, which may be thought of as a shock to the maximum packing concentration, plays a major role in determining the composition of the deposit and increases the average grain size relative to the initial suspension. It thus acts as a significant means of sorting the grains and segregating those of differing sizes.

3.2. Numerical Computations

[22] We now compare the predictions from our theoretical model to a series of experiments that investigated the settling behavior of polydisperse particle suspensions and their deposits [*Amy et al.*, 2006] by numerically integrating the coupled system of governing equations. The experiments were conducted in cylindrical settling tubes with a volume of 0.95 L, a height of 22.7 cm, and a diameter of 7.2 cm. The tubes were filled with approximately spherical glass ballotini and an aqueous saline solution in varying proportions. The grain-size distribution of the ballotini is shown in Figure 3a, and pertinent results are presented in Figures 3b–3g.

[23] The suspension in each tube was mixed with a stirrer and the tube was shaken vigorously. The tube was then inverted 20 times before being placed in an upright position. After 12 h had elapsed all the particles had completely sedimented out of suspension. The tube was then carefully placed, upright, in a freezer (−25°C) for a further 12 h, to freeze the deposits. The frozen deposits were split vertically, the thickness of the deposit was measured and samples along the centerline of the tube were taken for grain-size analysis. Grain-size analyses were conducted using a Malvern Mastersizer Micro. The experiments suggested three different, concentration-dependent deposition regimes (section 1).

[24] Figure 3 shows the direct comparison of experimental results [*Amy et al.*, 2006] with the theoretical calculations using the model presented above. The initial sediment distribution used in the experiments was arbitrarily discretized into particle classes each of 10 microns in width, resulting in 28 particle classes (Figure 3a). The numerical simulations of particle settling were allowed to run until sedimentation was complete, determined as when there was less than 10^{-3} % of the total initial volume fraction still in suspension. There was no direct fitting of numerical parameters to the experimental data aside from choosing the effective viscosity parameter $n = 5$ and the packing concentration $\phi_m = 0.6$ (see

Figure 3. (a) The initial distribution of grain sizes, $P(d)$, used in the experiments of *Amy et al.* [2006], discretized into 10 μm bins. (b-h) The composition of the deposit as a function of the normalized height within the deposit for different initial volume fractions, Θ. The experimentally measured (lines and symbols) and theoretically calculated (lines) profiles are shown for the 10th, 50th, and 90th percentiles of the grain size distribution. (Note the missing 10th percentile experimental data in Figure 3h.) Experimental error is estimated at 6%.

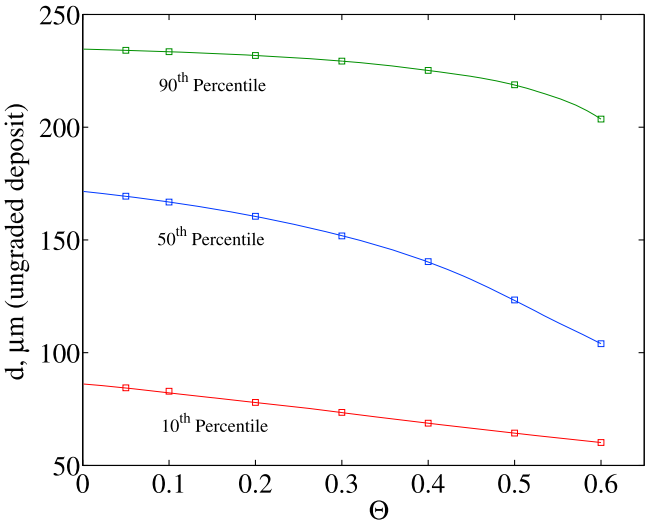

Figure 4. The 10th, 50th, and 90th percentiles within the ungraded deposit as a function of the initial volume fraction, Θ, for a suspension with the initial grain size distribution given by Figure 3a. The approximate solution (solid line) is plotted along with the complete numerical integration (squares) at initial volume fractions of 5%, 10%, 20%, 30%, 50%, and 60%.

section 2.1), and these values were then used for all of our computations without any further adjustment.

[25] After sedimentation was deemed to have finished, the 10th, 50th and 90th percentiles of grain size of the deposit were calculated, as will be discussed below. These are compared with the experimental results (L. Amy, personal communication, 2008). The experiments were subject to 6% error [*Amy et al.*, 2006] as shown by the error bars in Figures 3b–3h. The distinct stepping in the theoretical predictions of the grain size distribution is due to the discretization of the continuous suspension used in the experiments. This could be smoothed by dividing the initial distribution of grain sizes into more classes.

[26] The model results capture the general trends of the experiments well. Both the composition of the deposit and the depth at which deposit structure changes from ungraded to graded shows good quantitative agreement. The detailed structure of the graded region of the deposit is not of such good quantitative agreement, with the model predicting rather more rapid fining of average particle grain size with height than was observed in the experiments at high initial mass loadings.

[27] At higher concentrations, the predictions do not compare as well with the experimental results; see Figures 3e–3h. In this regime, it is difficult to mix the particles uniformly in the experimental configuration and to avoid clumping of particles. Also the MLB settling law (5) may be unsuitable when used at high concentrations. For example, *Selim et al.* [1983] and *Hoyos et al.* [1994] both found greater hindrance of large particles at high concentrations than predicted by the model used here. Additionally, the clumping of particles may create regions of high concentration and generate local instabilities associated with density anomalies that are not captured in this simple physical model. We note that such an effect ("elutriation pipes") was observed in one of the experiments conducted by *Amy et al.* [2006] at an initially high volume fraction ($\Theta = 0.5$).

3.3. Approximate Solutions for the Ungraded Deposit

[28] We now derive a simple, approximate expression for the average grain size within the ungraded portion of the deposit in terms of the initial characteristics of the overlying suspension. This approximation is based upon an assumed structure of the evolving form of the volume fraction of each species of particles.

[29] *Dorrell and Hogg* [2010] showed that for bidisperse suspension at very low and very high initial total volume fractions of particles, the volume fraction of each particle class above the deposit, ϕ_i^+, equal to its initial volume fraction. However, for intermediate mass loadings the volume fraction above the deposit had to be calculated by completely integrating the coupled governing equations for each species and thus it was not possible to relate the conditions in the suspension directly above the deposit simply to the initial conditions. For polydisperse suspensions, we now construct an approximate solution for the composition of the ungraded portion of the deposit, based upon the assumption that the volume fractions in the suspension above the deposit are equal to their initial conditions. As for the bidisperse suspensions, we anticipate that this approximation will be exact when the total mass loading is either very low or very high, but we demonstrate below that it appears to capture accurately the composition for all initial concentrations.

[30] On this assumption, we write

$$\phi_i^+ = P(d_i)\Theta, \tag{16}$$

where $P(d_i)$ is the initial grain size distribution within the suspension. (Figure 3a depicts the particular case examined in detail in this paper.) Thus, analogously to (12) and using the shock condition across the interface between the deposit and the suspension (7), we compute the average grain size within the deposit, $\overline{d^-}$, in terms of the initial distribution of grain sizes, the initial concentration of particles and the initial average grain size in the suspension, $\overline{d^+}$:

$$\overline{d^-} - \overline{d^+} = \frac{\phi_m - \Theta}{\phi_m(1-\Theta)} \cdot \left(\frac{\sum_{i=1}^{N} w_i d_i P(d_i) - \sum_{i=1}^{N} d_i P(d_i) \sum_{i=1}^{N} w_i P(d_i)}{\sum_{i=1}^{N} w_i P(d_i)} \right). \tag{17}$$

Since the settling velocity and the grain size are positively correlated, we immediately deduce that the mean grain size of the deposit decreases as the total concentration of the suspension approaches maximum packing ($\Theta \to \phi_m$).

[31] We may also use this approximation to determine the grain size within the deposit that corresponds to the 10th, 50th and 90th percentiles, and we compare these predictions against the output of the numerical model, when integrated from the initial distribution depicted in Figure 3a. The results are shown in Figure 4, where it is evident that the approximate solution accurately reproduces that computed by numerically integrating the system of coupled governing

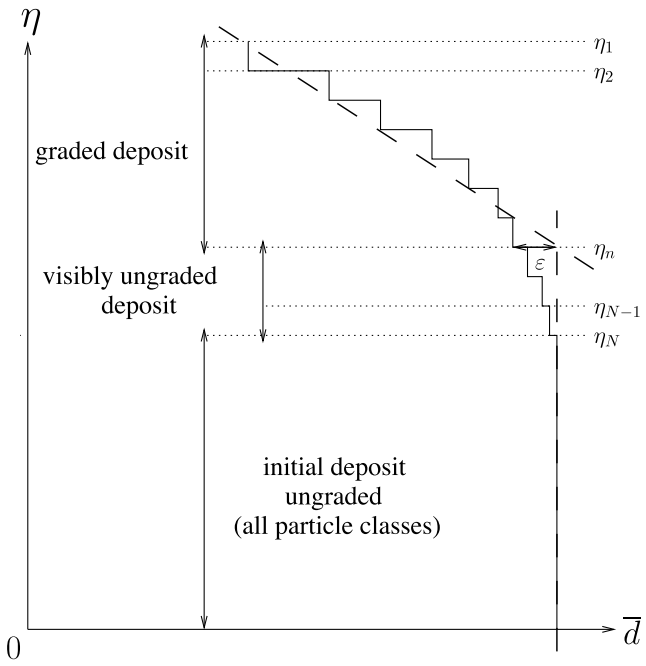

Figure 5. Schematic diagram of the deposit formed by a polydisperse suspension of N particle classes showing the initial deposit η_N, the end of the visibly ungraded deposit η_n, and the final deposit height η_1. Changes in grain size behavior in the deposit are exaggerated to highlight deposit structure.

equations. Figure 4 highlights the important result that there is approximately a 40% decrease of the median grain size within the ungraded portion of the deposit as the initial total volume fraction increases toward the maximum packing fraction. *Dorrell and Hogg* [2010] showed, for bidisperse suspensions, the dramatic impact on grading behavior of the deposit due to interior dynamics, such as upward propagating shocks in particle concentration, which form as a result of the mass conservation equations (as opposed to downward propagating shocks formed by differences in particle settling velocities). These interior dynamics increase the total concentration of the suspension before the shock to deposit. The good agreement between the approximate solutions and the full numerical solutions (Figure 4), suggests that the interior dynamics of polydisperse suspensions, such as upward propagating shocks in particle concentration, play a negligible role and that the approximation made earlier here is reasonable.

[32] We now calculate the depth of the deposit which contains particles from all the different particle classes η_N, under the aforementioned assumption that the suspension undergoes a simple shock to the maximum packing concentration, such that ϕ_i^+ before the shock to the deposit is equal to $P(d_i)\Theta$ (16). The depth η_N, is found by equating the location of the falling interface γ_N, of the fastest sedimenting particle with settling velocity W_N,

$$\gamma_N = h - (1-\Theta)^{n-1}\left(w(d_N) - \sum_{i=1}^{N}\Theta P(d_i)w(d_i)\right)t,$$

where d_N is the diameter of the largest particle class from the suspension, with the depth of the deposit

$$\eta_N = \frac{\sum_{i=1}^{N}\Theta P(d_i)\left(w(d_i) - \sum_{j=1}^{N}\Theta P(d_j)w(d_j)\right)}{(1-\Theta)^{1-n}(\phi_m - \Theta)}t$$

$$= \frac{(1-\Theta)^n\Theta}{\phi_m - \Theta}\sum_{i=1}^{N}P(d_i)w(d_i)t.$$

Thus, we find that η_N is given by

$$\eta_N = \frac{h(1-\Theta)\sum_{i=1}^{N}\Theta P(d_i)w(d_i)}{(\phi_m - \Theta)w(d_N) + (1-\phi_m)\sum_{i=1}^{N}\Theta P(d_i)w(d_i)}. \quad (18)$$

From this equation we note that $\eta_N = 0$ when $\Theta = 0$ and in the limit of $\Theta \to \phi_m$, $\eta_N \to h$, as is to be expected. Further, since $w(d_N) > \sum_{i=1}^{N} P(d_i)w(d_i)$, we find that η_N increases monotonically with Θ in the range $0 < \Theta < \phi_m$. As shown in Figure 5 the next layer of the deposit ($\eta_N < z < \eta_{N-1}$) consists of all but the largest class of particles. It follows that the mean grain size in the deposit between η_N and η_{N-1} must decrease as the largest class of particles has been completely deposited. Following this argument we can build up the entire deposit structure as a series of steps in grain size behavior, η_N, η_{N-1} … η_2, η_1, where η_1 is the top of the deposit. The ungraded deposit depth, χ, is thus given by η_N/η_1.

[33] After the largest particle class has been completely deposited, the mean grain size starts to decrease, however this initial variation may be small, especially if only a relatively small fraction of the total mass is contained within these classes of particles of the largest diameters. We propose that by fitting two straight lines through the mean grain size of the deposit, one through the strongly graded, upper, region of the deposit and one through the deposit between 0 and η_N as in Figure 5, that the intersection of the two gradients approximates the height where the deposit becomes visibly graded, η_n. For heights $\eta_N < z < \eta_n$ the mean diameter differs from that in the ungraded portion of the deposit by less than ϵ (see Figure 5). This empirical division splits the deposit into three regions: 0 to η_N being ungraded, η_N to η_n, which is slightly graded and captures the initial weak fining behavior of the deposit and η_n to η_1 which captures the strongly graded behavior of the top of the deposit.

4. Discussion

[34] The theoretical model provides an accurate prediction of the composition of the deposit measured experimentally by *Amy et al.* [2006] for a range of initial concentrations. The experimental deposits have two key features. Firstly, they have a basal ungraded region overlain by a strongly graded region. Secondly, the normalized thickness of the ungraded region increases as the initial concentration of the suspension is increased. In the following paragraphs an explanation of these features based on the model is provided. For simplicity all particles are considered to have the same density and therefore larger particles have faster settling velocities.

[35] As settling begins from an initial uniformly mixed suspension, $N + 2$ distinct regions form within the suspen-

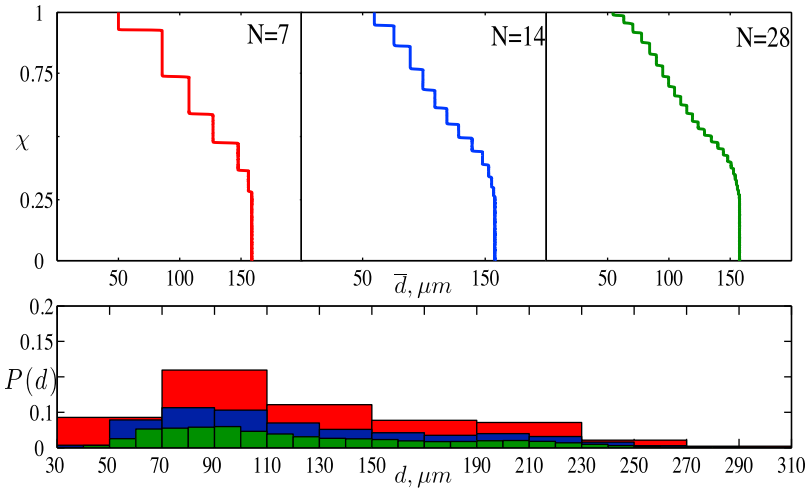

Figure 6. The dependence of deposit structure on the number of particle classes, showing the mean grain size of a deposit and initial particle distribution for a suspension of initial volume fraction $\Theta = 0.3$, where the total number of particle classes are $N = 7$, $N = 14$, or $N = 28$.

sion, where N is the number of particle classes. At the bottom there is a stationary deposit, in which the concentration of particles is at maximum packing. The deposit is overlain by a region that contains particles of all sizes present in the initial suspension. Each successive region, with increasing height in the suspension, is devoid of the largest particle class from the region below. At the top of the suspension there is a region that only contains particles of the smallest class; this region is overlain by clear fluid. The fall velocity of the interface between any two regions emerges as a shock in the concentration field of the largest particle class below it varies discontinuously and vanishes above the interface. It may be shown therefore the velocities of the interfaces $\gamma_1,\ldots,\gamma_N$ (see Figure 1) are the hindered settling velocities of the largest particle present in the region below the interface.

[36] In the model the ungraded part of the deposit is a result of a constant mass flux of particles and its constant composition into the deposit until all of the largest-size class of particles has been deposited. In terms of the schematic Figure 1, this occurs when the settling interface, γ_N, intersects with the growing deposit. During this period, particles of all sizes are present in the suspension and while the flux of particles into the deposit is constant, the mean grain size of particles being deposited does not change. Despite different sized particles falling at different velocities, the mass flux into the deposit is constant, because the bed can be shown to form a rising interface along which concentration is constant [cf. *Dorrell and Hogg*, 2010; *Dorrell*, 2010]. This implies that the concentrations of each particle class remain constant above the deposit suspension interface, resulting in a constant mass flux of each species within a localized region of the suspension.

[37] The position of the top of the ungraded region of the deposit, η_N, is defined as the height at which the rising deposit interface and the lowermost falling interface meet (Figure 5). The position of this falling interface is determined by the hindered settling velocity of the largest particle in the lowermost region, which in turn depends on the initial conditions of all of the particle species. Thus, as the total initial concentration of the suspension, Θ, increases then the settling velocity of the largest particle will decrease. Although the rate of rise of the interface that marks the top of the deposit does not vary monotonically with Θ, its variation is dominated by that of the falling interface and thus the depth of the ungraded layer increases monotonically with Θ. (This may be deduced from (18), noting that $w(d_N) > \sum_{i=1}^{N} P(d_i)w(d_i)$.) This means that the ungraded portion of the deposit encompasses a greater proportion of the overall particulate load with increasing Θ and thus its composition, which is vertically uniform, progressively fines with increasing Θ. Also this implies that the normalized depth of the ungraded region of the deposit increases as the initial concentration of the suspension is increased as it contains a larger proportion of the particle distribution initially in suspension.

4.1. The Dependence of the Model on the Number of Particle Classes

[38] One seemingly arbitrary feature of the results computed in this study is the number of discrete classes of particles into which the suspension is divided. In section 3.2, we calculated results for $N = 28$, but other discretizations could have been made, which affect the number of internal interfaces formed (see section 2.1) and the interpretation of the ungraded portion of the deposit (section 3). We investigate numerically the effects on the computed deposits of having sampled the suspension using fewer classes of particles, by integrating the governing equations from initial conditions to final deposit formation with $N = 7$, 14, and 28.

[39] Figure 6 shows a comparison between the deposit generated from three different numerical simulations of a settling suspension with an initial 30% volume fraction of sediment, each simulation being run with a different number of particle classes. From Figure 6 it is evident that the initial average grain size of the deposit, $\overline{d}$, varies only weakly when the bin size of the particle classes is doubled or quadrupled. Similarly the depth of the ungraded region of the deposit, η_N, varies only weakly with the resolution of the grain size distribution. However it is apparent that there is an

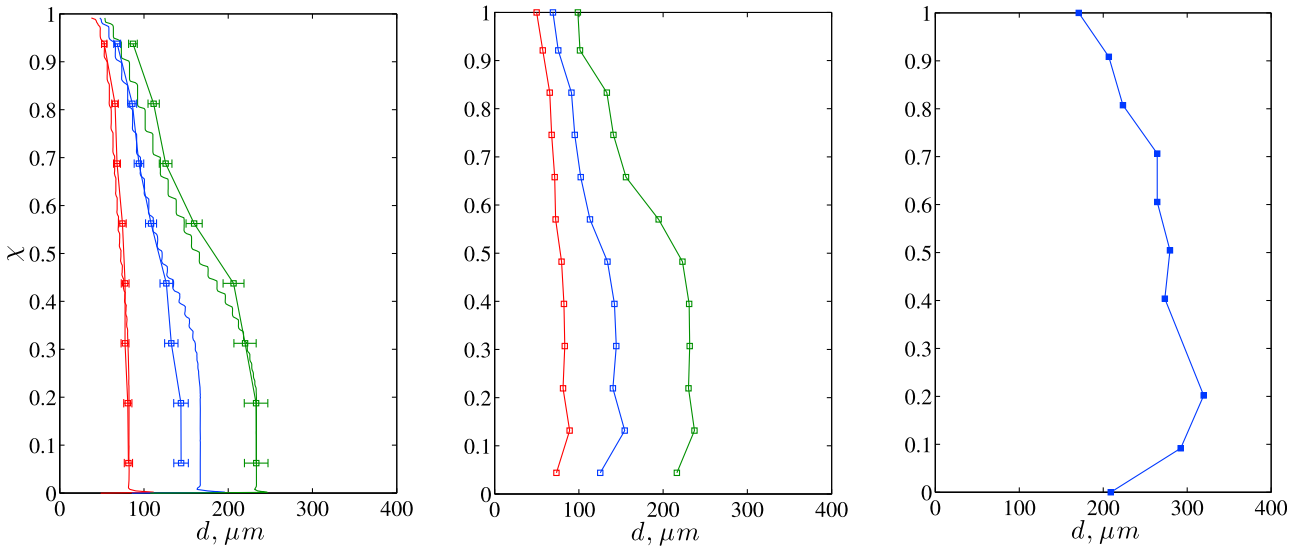

(a) Static Settling (b) Decelerating Flow (c) Turbidite Deposit

Figure 7. (a) Experimental and theoretical results of the settling tube experiment, Figure 3c. (b) Grain size of a deposit generated in an annular flume containing a suspension of particles at an initial volumetric concentration of 10%, decelerated from 3.5 m s^{-1} to rest over 420 s [see *Sumner et al.*, 2008, Figure 7E]. (c) Mean grain size of the deposit of a turbiditic sandstone from Flysch di Motta, Miocene, southwest Calabria, Italy, redrawn from *Baas* [2004, Figure 1.]

change in the "roughness" in the graded region of the deposit, where the solution is broken down into a number of discrete steps, which each equate to an individual particle class.

[40] We may explain the relative invariance of η_N and $\overline{d}$ when varying the number of particle classes by using (12) and (14). There we showed that the expression for $\overline{w^-}$ depends not only on the average settling velocity, $\overline{w^+}$, but also on the average of the square of the settling velocity, $\overline{w^{+2}}$. Increasing the sampling bin size will preserve $\overline{w^+}$, but will generally increase $\overline{w^{+2}}$. However, because there are relatively few particles of the very largest diameters, the increase will not be very large. Thus, we find that the mean grain size in the ungraded portion of the deposit and its depth are relatively unchanged.

4.2. Insights Into Turbidity Currents and Their Deposits

[41] Finally, we suggest some possible relevance of these results to the deposits formed from submarine turbidity currents. Evidently settling plays a significant role in turbidity currents as the sediment is laid down in the deposit. However, there are a number of important features that differ between the settling tube experiments [*Amy et al.*, 2006], the models developed here and the dynamics of turbidity currents. Notably, both the modeling and experiments do not simulate streamwise (and lateral) advection of sediment, reworking of sediment as bed load, turbulent suspension and resuspension from the bed, more complex deceleration or acceleration patterns and the effects of mud on the turbulence and the settling dynamics.

[42] Some of the processes may be dynamically insignificant. For example, sediment resuspension from the bed will be minimal if the bed aggradation rate is rapid, as would the degree of bed load reworking. Mud can influence flow structure by damping turbulence and can potentially support sand through a finite yield strength [*Baas et al.*, 2009; *Sumner et al.*, 2009]. However the sediment considered here and used in the experiments conducted by *Amy et al.* [2006] was cohesionless spherical glass beads. The modeling and experiments therefore may most closely simulate the basal part of flows in which there is rapid deposition, the turbulence-induced flux of particles is negligible relative to the settling flux and there is an initially uniform suspension. Under these restricted conditions we note that the suspensions can form weakly graded deposits from relatively high initial concentrations and that the thickness of the deposit provides an indication of the concentration within the parent flow.

[43] In Figure 7, we plot the variation of grain size within the deposit for the setting experiments [*Amy et al.*, 2006] and the theory developed in this paper; experiments conducted with sedimenting suspensions within a decelerating annular flume [*Sumner et al.*, 2008]; and from field data of turbiditic sandstone [*Baas*, 2004]. It is intriguing to note that they share rather common features. The experimental studies within the annular flume were conducted with suspensions with the same initial characteristics as those used by *Amy et al.* [2006] and considered here, which were decelerated from relative high velocities (~3 m s^{-1}) to rest over periods ranging from 10 to 900 s during which the particles settled out of suspension and formed the deposit. The sedimentation processes that occur in these experiments are closer to those in a turbidity current than the settling tube experiments of *Amy et al.* [2006] because they include streamwise advection of sediment, reworking of sediment as bed load and turbulent suspension. It is intriguing, therefore,

that the deposits formed from the decelerating flows show surprisingly similar structures to the deposits produced in the settling tube experiments and it is suggestive that they may share the same underlying physical processes that have been elucidated in this paper. We also note that the same generic structure in the deposit appears in many field measurements [see, e.g., *Baas*, 2004], featuring a region with weak normal grading overlain by rapid normal grading). These similarities in the grading patterns are suggestive that when the flow is depositional, the sedimentation processes are only weakly modified by shear in the suspending fluid. However, this conclusion requires further justification to extend our results, which have quantitatively modeled hindered settling and deposit formation in otherwise quiescent fluid, to situations in which the interstitial fluid is in motion.

5. Conclusions

[44] We have presented a quantitative model of particle settling from an otherwise quiescent suspension, which can be integrated from an initial state with all the classes of particles in suspension to a final state in which they have all been deposited. This allows the composition and structure of the deposit to be related to the initial characteristics of the overlying suspension. We have compared the theoretical predictions to the experimental measurements [*Amy et al.*, 2006] and have shown that the model is able to reproduce accurately many features such as the depth of the ungraded portion of the deposit and its average grain size. The model was not adjusted empirically to attain this quantitative agreement. An important result that emerges is that the interface between the deposit and the overlying suspension should be treated as a shock over which the volume fractions of all of the species of particles vary discontinuously. It was established that the rate of growth of the ungraded portion of the deposit and its composition remain constant until the largest class of particles has completely settled out and that this discontinuity always leads to an increase in the mean grain size, relative to the overlying suspension. Also, the relative extent of the ungraded portion of the deposit increases and the difference between average grain size in the deposit and the suspension diminishes as the initial concentration of the suspension increases. Indeed we have shown that deposits with relatively thick ungraded bases can form under settling suspensions when the initial concentration is sufficiently high and this implies that the effects of hindered settling may be nonnegligible in many depositing flows.

[45] **Acknowledgments.** This work was supported by the Natural Environment Research Council (NER/S/A/2006/14067). Lawrence Amy is thanked for providing the data from the original laboratory experiments. Mark Woodhouse is thanked for constructive comments. Additionally, three anonymous referees are thanked for their careful reviews and suggestions for improvements on an earlier draft of this work.

References

Amy, L. A., and P. J. Talling (2006), Anatomy of turbidites and linked debrites based on long distance (120 × 30 km) bed correlation, Marnoso Arenacea Formation, Northern Apennines, Italy, *Sedimentology*, *53*(1), 161–212, doi:10.1111/j.1365-3091.2005.00756.x.

Amy, L. A., P. J. Talling, V. O. Edmonds, E. J. Sumner, and A. Lesueur (2006), An experimental investigation of sand-mud suspension settling behaviour: Implications for bimodal mud contents of submarine flow deposits, *Sedimentology*, *53*(6), 1411–1434, doi:10.1111/j.1365-3091.2006.00815.x.

Baas, J. H. (2004), Conditions for formation of massive turbiditic sandstones by primary depositional processes, *Sediment. Geol.*, *166*, 293–310, doi:10.1016/j.sedgeo.2004.01.011.

Baas, J. H., J. L. Best, J. Peakall, and M. Wang (2009), A phase diagram for turbulent, transitional, and laminar clay suspension flows, *J. Sediment. Res.*, *79*, 162–183, doi:10.2110/jsr.2009.025.

Batchelor, G. K. (1967), *An Introduction to Fluid Dynamics*, 615 pp., Cambridge Univ. Press, Cambridge, U. K.

Batchelor, G. K. (1982), Sedimentation in a dilute polydisperse system of interacting spheres. Part 1. General theory, *J. Fluid Mech.*, *119*, 379–408, doi:10.1017/S0022112082001402.

Bürger, R., A. Garcia, K. H. Karlsen, and J. D. Towers (2008), A family of numerical schemes for kinematic flows with discontinuous flux, *J. Eng. Math.*, *60*(3–4), 387–425, doi:10.1007/s10665-007-9148-4.

Davis, R. H., and A. Acrivos (1985), Sedimentation of noncolloidal particles at low Reynolds numbers, *Annu. Rev. Fluid Mech.*, *17*, 91–118, doi:10.1146/annurev.fl.17.010185.000515.

Davis, R. H., and H. Gecol (1994), Hindered settling function with no empirical parameters for polydisperse suspensions, *AIChE J.*, *40*(3), 570–575, doi:10.1002/aic.690400317.

Dietrich, W. E. (1982), Settling velocity of natural particles, *Water Resour. Res.*, *18*(6), 1615–1626, doi:10.1029/WR018i006p01615.

Dorrell, R. M. (2010), Particulate suspensions: The mechanisms of suspensions and deposition, Ph.D. thesis, 240 pp., Univ. of Bristol, Bristol, U. K.

Dorrell, R. M., and A. J. Hogg (2010), Sedimentation of bidisperse suspensions, *Int. J. Multiphase Flow*, *36*, 481–490, doi:10.1016/j.ijmultiphaseflow.2010.02.001.

Gladstone, C., and R. S. J. Sparks (2002), The significance of grain-size breaks in turbidites and pyroclastic density current deposits, *J. Sediment. Res.*, *72*, 182–191, doi:10.1306/041801720182.

Hoyos, M., J. C. Bacri, J. Martin, and D. Salin (1994), A study of the sedimentation of noncolloidal bidisperse, concentrated suspensions by an acoustic technique, *Phys. Fluids*, *6*, 3809–3817, doi:10.1063/1.868372.

Kansal, A. R., S. Torquato, and F. H. Stillinger (2002), Computer generation of dense polydisperse sphere packings, *J. Chem. Phys.*, *117*, 8212–8218, doi:10.1063/1.1511510.

Kynch, G. J. (1952), A theory of sedimentation, *Trans. Faraday Soc.*, *48*(2), 166–176, doi:10.1039/tf9524800166.

Lockett, M. J., and K. S. Bassoon (1979), Sedimentation of binary particle mixtures, *Powder Technol.*, *24*, 1–7, doi:10.1016/0032-5910(79)80001-7.

Masliyah, J. H. (1979), Hindered settling in a multi-species particle system, *Chem. Eng. Sci.*, *34*(9), 1166–1168, doi:10.1016/0009-2509(79)85026-5.

Richardson, J. F., and W. N. Zaki (1954), The sedimentation of a suspension of uniform spheres under conditions of viscous flow, *Chem. Eng. Sci.*, *3*(2), 65–73, doi:10.1016/0009-2509(54)85015-9.

Selim, M. S., A. C. Kothari, and R. M. Turian (1983), Sedimentation of multisized particles in concentrated suspensions, *AIChE J.*, *29*, 1029–1038, doi:10.1002/aic.690290623.

Shapiro, A. P., and R. F. Probstein (1992), Random packings of spheres and fluidity limits of monodisperse and bidisperse suspensions, *Phys. Rev. Lett.*, *68*, 1422–1425, doi:10.1103/PhysRevLett.68.1422.

Soulsby, R. (1997), *Dynamics of Marine Sands: A Manual for Practical Applications*, Thomas Telford, London.

Sumner, E. J., L. A. Amy, and P. J. Talling (2008), Deposit structure and processes of sand deposition from decelerating sediment suspensions, *J. Sediment. Res.*, *78*(8), 529–547, doi:10.2110/jsr.2008.062.

Sumner, E. J., P. J. Talling, and L. A. Amy (2009), Deposits of flows transitional between turbidity and debris flows, *Geology*, *37*(11), 991–994, doi:10.1130/G30059A.1.

Sylvester, Z., and D. R. Lowe (2004), Textural trends in turbidites and slurry beds from the Oligocene flysch of the East Carpathians, Romania, *Sedimentology*, *51*(5), 945–972, doi:10.1111/j.1365-3091.2004.00653.x.

Talling, P. J., L. A. Amy, and R. B. Wynn (2007), New insight into the evolution of large-volume turbidity currents: comparison of turbidite shape and previous modelling results, *Sedimentology*, *54*(4), 737–769, doi:10.1111/j.1365-3091.2007.00858.x.

R. M. Dorrell and A. J. Hogg, Centre for Environmental and Geophysical Flows, School of Mathematics, University of Bristol, University Walk, Bristol BS8 1TW, UK. (a.j.hogg@bristol.ac.uk)

E. J. Sumner and P. J. Talling, National Oceanography Centre, University of Southampton, Waterfront Campus, European Way, Southampton SO14 3ZH, UK.